Hindawi
Advances in Civil Engineering
Volume 2022, Article ID 1964903, 11 pages
https://doi.org/10.1155/2022/1964903

Research Article

Analysis of Lightweight Polystyrene Foam Concrete Flat Slabs under Fire Condition

Majed Alzara,[1] Magdy Riad,[2] Mohamed AbdelMongy,[1,3] Mohamed A. Farouk,[4] Ahmed M. Yosri,[1,4] Ahmed M. Moubarak,[4] and Ahmed Ehab[5]

[1]*Department of Civil Engineering, Jouf University, Sakakah, Saudi Arabia*
[2]*Civil Engineering Department, Higher Institute of Engineering, El Shourouk Academy, El Shorouk, Egypt*
[3]*Civil Engineering Department, Faculty of Engineering, Al-Azhar University, Cairo, Egypt*
[4]*Civil Engineering Department, Faculty of Engineering, Delta University for Science and Technology, Belkas, Egypt*
[5]*Department of Civil Engineering, Badr University in Cairo, Badr, Egypt*

Correspondence should be addressed to Ahmed M. Yosri; engineering@ju.edu.sa

Received 12 November 2021; Revised 8 May 2022; Accepted 21 May 2022; Published 22 June 2022

Academic Editor: Giovanni Garcea

Lightweight reinforced concrete (LWC) is widely used in various reinforced concrete (RC) applications, such as its use in diverse types of reinforced concrete slabs. The aim of this study is to analyze the behavior of reinforced foam concrete slabs (flat slab type) that are exposed to fire conditions under the influence of eccentric loads as well as concentric loads. This analysis has been done using the finite element method by a (ANSYS) software program. The validity of the adopted models was verified through comparison with a previous experimental study. The studied specimens were eleven reinforced concrete flat slabs with a thickness of 150 mm. The lightweight polystyrene foam concrete was used in these specimens with a density of 1820 kg/m^3. The results showed that the fire effect lead to a decrease in the maximum carrying load of foam concrete slabs by 25%. Also, by comparing the finite element results with the selected experimental study, the results showed a great agreement with the analytical study used in this research.

1. Introduction

The use of lightweight concrete has been widespread since the 18th century. There was a necessary need to use this type of concrete to reduce the cost of reinforced concrete structures. Looking at the main factors that have effects on reducing the weight and density of concrete, the weight and type of the aggregate used as well as the ratio between coarse aggregate and fine aggregate are the main factors that can be used for this purpose.

It is also possible to use foam in its various forms in mixed concrete materials in order to produce the lightweight concrete. Numerous and varied studies have dealt with the use of foam in the production of lightweight concrete. Due to the availability of manufacturing foam of different types in many countries, it can be used in a simple way to produce this type of concrete. In 2014, M. Tech Scholar [1] have made an analytical study of two mixtures of foam concrete, the first mixture of foam concrete with sand and the second mixture without sand, and the study dealt with many experiments to determine the proportions of the concrete mixture to reach a density of 1900 kg/m^3. This study concluded that the ratio of the mixture which is used in the study is not suitable for the production of foam concrete which can be used in structural purposes because the compressive strength resulting from the concrete was less than 17.0 MPa, after 28 days of casting.

Helal et al. [2] conducted a practical study for the purpose of improving the preformed foam concrete, which was produced with a density of 1300 to 1900 kg/m^3. This study relied on the use of two types of materials that are added to concrete (fly ash and silica fume) in addition to use of a water reducing agent. The results of this study were good, as these materials showed a clear improvement in the structure of concrete pores, as well as an increase in strength, in addition to a reduction in concrete's absorption of water. The results also showed that these materials had slightly increased the thermal conductivity of concrete.

According to the study conducted by Wan Ibrahim et al. [3], the effect of polyolefin fibers on the properties of foam concrete was studied (such as flexural strength and compressive strength). The density of concrete that is used in this study ranged from 1300 to 1600 kg/m^3. The researchers used in the study polyolefin sized fibers at relatively low volume fraction with percentages ranging from 0.0%, 0.20%, 0.40%, and 0.60%. The results of the study were that the compressive strength and flexural strength of foam concrete were slightly affected as a result of using the mentioned fibers by 4.3% and 9.3%, respectively.

Also, the researchers of Lee et al. (2017) [4] have conducted their study on slabs and beams of foam concrete, which was produced using a type of lightweight foam mortar, and the density of concrete ranged from 1700 to 1800 kg/m^3. Accordingly, the concrete's compressive strength was 20 MPa. The results of this study were that the mortar used led to a decrease in the maximum load from 8.0% to 34.0%, when compared to that of reinforced concrete with natural density using the same type of mortar.

By reviewing the reviews and previous studies, it was found that foam concrete can be used successfully in reinforced concrete structures by using additives and different types of fibers. Concrete slabs made of structural polystyrene foam can be used to replace hollow block panels and thermally insulated layers.

Several design models were developed for punching shear strength; however, these models vary significantly in the considered parameters and mechanisms in developing the model [5–9]. For example, the European concrete design code (EC2) [5] model is semiempirical. In contrast, the FIB model design code (MC) [6] is physically based. Thus, there are many reviews that have studied the performance of flat slabs when exposed to fire. References [10–18]. Despite the diversity of these studies, it was noted that the behavior of polystyrene foam concrete when exposed to fire was not studied.

El-Fitiany and Youssef [13] in their study conducted a simple method to predict the flexural and behavior of reinforced concrete sections during exposure to high temperatures. This proposed method was validated experimentally by an analytical study. Wang [14] experimentally studied the structural behavior of reinforced foam concrete flat slab exposed to fire under diverse loading such as concentric and eccentric. The eleven flat slab specimens with square dimensions of 1750 mm length and 150 mm thickness were tested. The central column with a square cross section 200 × 200 mm was located at the center of each slab. The results in that study showed that the maximum load of the specimens with light weight foam concrete were reduced compared to those of specimens with normal concrete.

The main purpose of this study is to identify the efficiency of structural lightweight polystyrene foam concrete flat slabs under varies parameters when these slabs are exposed to fire.

2. Materials and Methods

The validity of the adopted models was verified through a comparison with a previous experimental study which was conducted by Riad and Shoeib [18]. In their study, two concrete mixes were used, one for the light weight concrete specimens and another mix was for the normal concrete specimens. Polystyrene foam, silica fume, and super plasticizer were used in the mix in order to achieve the self-compacting lightweight concrete; also, fine crushed stone of nominal maximum size of 10 mm was used as a coarse aggregate. Steel rebars with grades (240/350) and (360/520) were used. The yield strength and ultimate tensile strength for a mild steel (240/350) were (240 MPa) and (350 MPa), respectively, and this steel was 8 mm in diameter. The proof strength of high tensile steel deformed rebars with grade (360/520) was 360 MPa and ultimate tensile strength of these were 520 MPa. This rebars with bar sizes of (12 mm) and (16 mm).

3. Numerical Program

3.1. Numerical Specimens and Parameters. The numerical specimens included eleven tested RC simply supported square slabs with typical dimensions of 150 mm thickness and 1750 mm length. The clear span was equal to 1650 mm. The RC column is square with 200 mm in the case of the concentric load. In the case of an eccentric load, the column was extended above the slab compression face by 200 mm for all tested specimens. The typical concrete specimen's dimensions and reinforcement details are shown in Figure 1 as the experimental specimens that are presented by Riad and Shoeib [18].

The main parameters in this work are the effect of the percentage of tension steel reinforcement (0.40% and 0.70%) and type of vertical loads (concentric or eccentric) on the performance of flat slab when exposed to fire. Five specimens with normal-weight concrete and six specimens with polystyrene foam concrete slab have been tested.

The eleven tested specimens are divided into four groups as shown in Figure 2 and as follows:

(i) The first group (3 control specimens) studies the behavior of normal-weight concrete with different load types and steel ratios.

(ii) The second group (2 specimens) studies the behavior of normal-weight concrete exposed to fire from 0 to 500°C and is loaded by 30% of the ultimate with gradual increasing to ultimate load after cooling by air.

(iii) The third group, (3 specimens), and considers the effect of the load type and main steel ratios on the behavior of lightweight concrete

(iv) The fourth group (3 specimens) is similar to the second group but by using lightweight concrete instead of the normal concrete.

3.2. Modeling Slabs by ANSYS. This section presents elements types, real constant, material properties, numerical concepts, boundary conditions, and analysis types so as process together with load stepping.

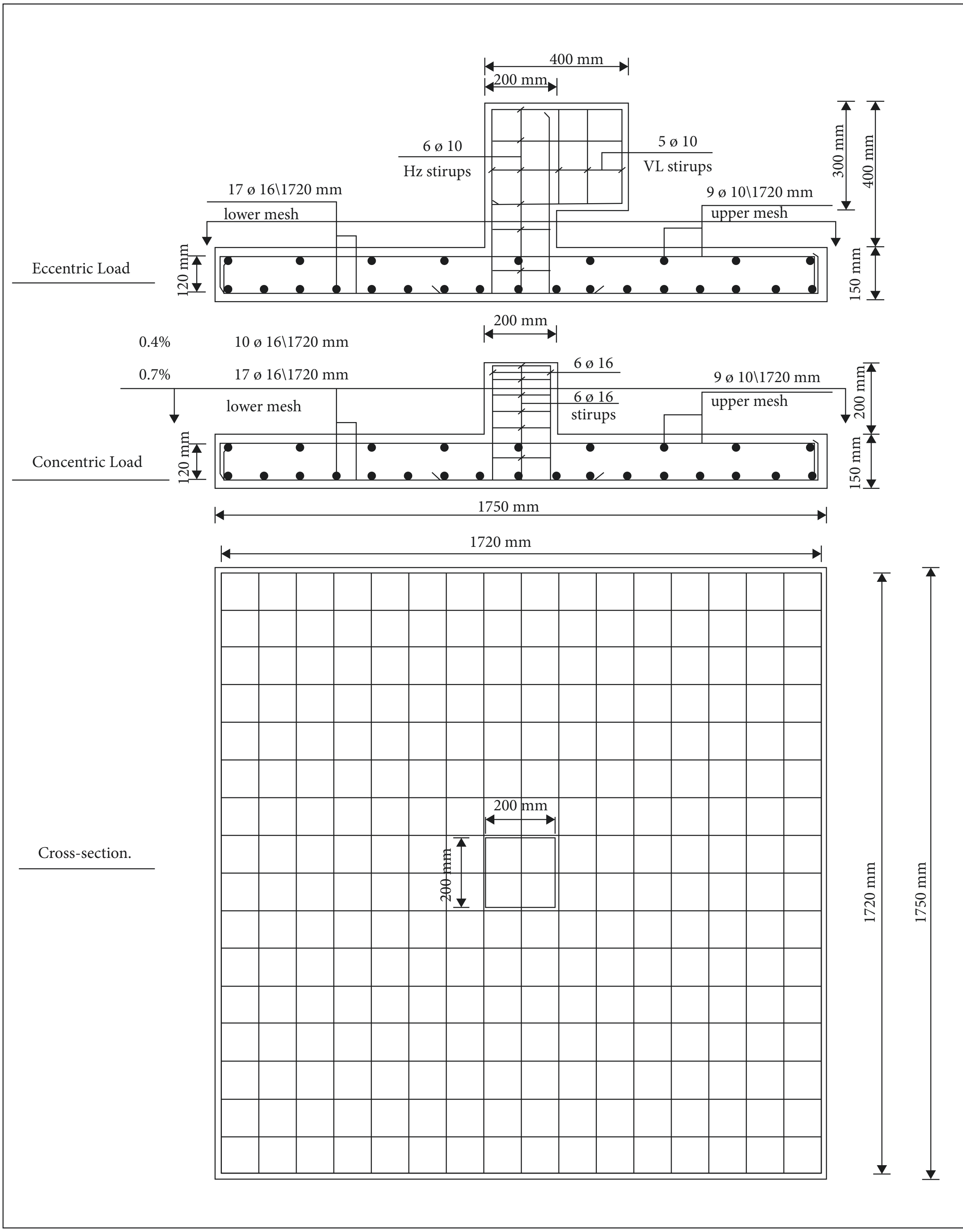

Figure 1: Typical dimensions and RFT for tested specimens.

3.2.1. Elements Types. There are mainly four elements used at the analysis; the names, shapes, number of degree of freedom, and some properties are shown below in Table 1.

3.2.2. Loads and Boundary Conditions. Similarly, for the experimental slabs, all joints at the border of the slab are modeled as a simply supported, which was constrained in the *UY*. Two nodes in the *X* direction are constrained in the

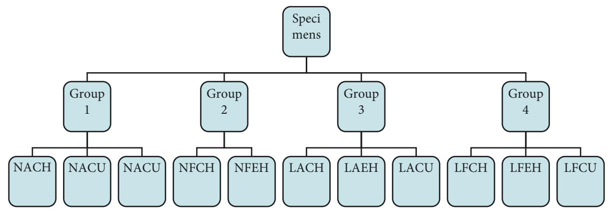

Figure 2: Main groups of specimens. N^* normal-weight concrete (NWC), L^* lightweight concrete (LWC), A^* without fire, F^* exposed to fire, C^* under concentric load, E^* under eccentric load, U^* 0.4% Rft (Reinforced steel ratio) from gross area of slab, and H^* 0.7% Rft from gross area of slab.

Table 1: Summary for the elements needed at modeling.

Properties\element	Concentric element		Steel reinforcement element	Lead Plate and Supports
Name	Solid65 (structural concentric element)	Solid75 (thermal concentric element)	Link180	Solid185
Shape	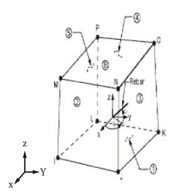	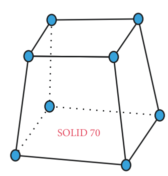	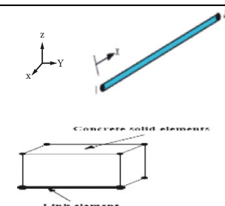	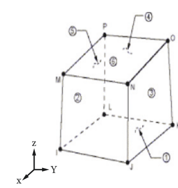
No. of nodes	8	8	3	8
Properties	1-capable of plastic-deformation 2-cracking in 3-orthogonal direction 3-crushing	1-having thermal degree-of-freedom 2-using at heat condition	1-Proficient in plastic-deforcement 2-connected between nodes 3-2 materials share the same nodes	1-Plastic and hyper-elastic 2-allows for stress-stiffening 3-creep so as large deflection together with large strain

UX and another two nodes, in the *Y* direction *UY*. The displacement is applied at the column head based on its position. The displacement is applied at a single node on upper plate using the incremental displacement method. The support and the displacement applied are presented in Figure 3.

4. Verification of the Analytical Model

Table 2 shows the verification of the analytical model and experimental slabs which was tested by Riad and Shoeib [18]; the table divided into two main categories related to the output of the analysis. The first category shows the failure loads for each specimen at experimental and analytical models and the percentage of difference between both. The second category is the same but for the deflection at edge of column.

4.1. Crack Patterns and Load-Deflection Curves. Table 3 shows the propagation of cracks of the slabs specimen 1, 3, 6, and 8 just before failure using the finite element model and actual failure shape and load–deflection curves.

4.2. Parametric Study and Effect of Eccentricity on the Behavior of a Flat Slab. To study the effect of eccentricity on the behavior of lightweight concrete, the specimens are divided to four groups, each group includes eight specimens related to the ratios of steel (0.4 and 0.7 which are called *U* and *H*, respectively), the eccentricity which varies from 0.5 to 1 with a 25% increasing fixed percentage, type of concrete, and heating intensity or temperature are as shown in the table below. Table 4 has been expressed as a database at the nonlinear finite element analysis for the same slab cross section and steel grade as the experimental program.

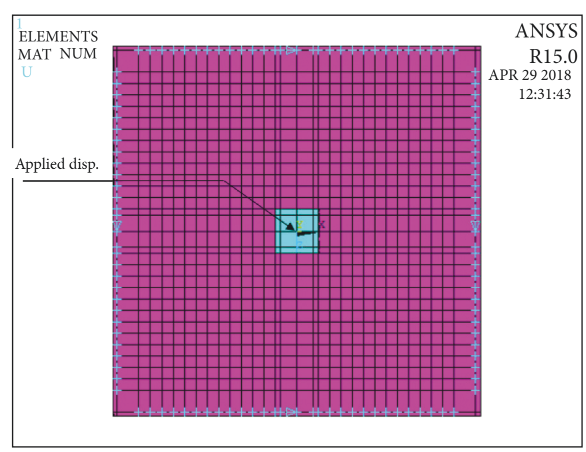

Figure 3: Support condition and applied displacement.

4.3. Parametric Study Database Analysis and Results. A nonlinear finite analysis is conducted using ANSYS software, to

Table 2: Verification of the analytical model and tested specimens of Riad and Shoeib [18].

Group	Specimen	Specimens code	Failure load (kN)			Deflection at edge of column (mm)		
			Experimental	Analytical	% diff.	Experimental	Analytical	% diff.
G1	S1	NACH	462	483.7	4.7	13.92	13.4	−3.74
	S2	NAEH	382	417.6	9.3	12.3	11.65	−5.28
	S5	NACU	383	396.95	3.64	15.1	14.67	−2.85
G2	S3	NFCH	444	451.23	1.65	15.15	17.43	15.0
	S4	NFEH	298.7	311.73	4.36	15	14.85	−1.0
G3	S6	LACH	430	459.7	6.9	17.72	16.04	−9.48
	S7	LAEH	367	406.4	10.73	11.4	12.28	7.71
	S11	LACU	343	376.6	9.8	15.5	14.55	−6.13
G4	S8	LFCH	332	341.33	3	19.75	19.44	−1.57
	S9	LFEH	238	272.24	14.38	14.33	13.23	−7.68
	S10	LFCU	278	286.7	3.13	15.9	15.95	0.5

2. N^* normal-weight concrete, L^* lightweight concrete, A^* without fire, F^* exposed to fire, C^* under concentric load, E^* under eccentric load, U^* 0.4% rft from gross area of slab, H^* 0.7% rft from gross area of slab.

Table 3: Summary of finite element models, cracks, and load-deflection curves.

Sample	Finite element model	Crack	Load-deflection
S1 (NACH)	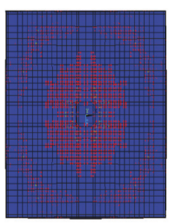	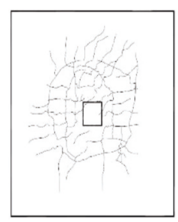	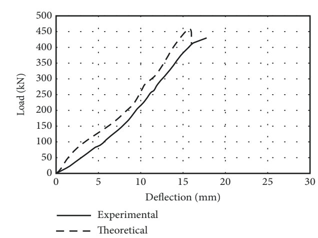
S3 (NFCH)	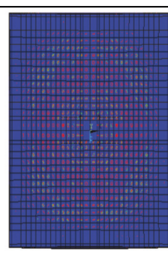		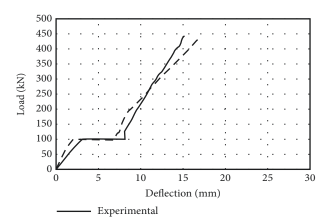
S6 (LACH)	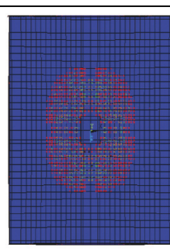		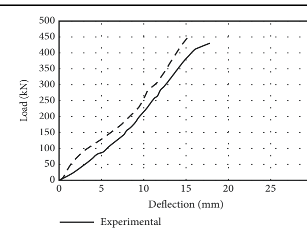
S8 (LFCH)	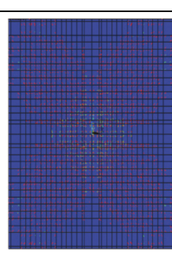		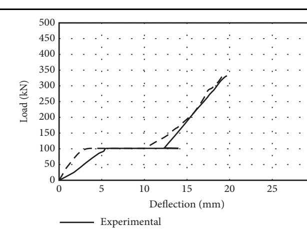

predict the ultimate loads and deflection for the constructed parametric study database. The finite element predicted failure loads and deflection at edge of column. Figure 4 presents the crack propagation before ultimate from the finite element model.

In case of the study of the behavior of lightweight RC, flat slabs with RFT percentages equal to 0.7% and 0.4% when applying the concentric and changing eccentric vertical load $e/t = 0.5$, 0.75 and 1.0.

Table 4: Parametric study database of slabs.

Group	Specimens	Specimens code	Type of concrete	Heating temp (C°).	Eccentricity ratio ($e\backslash t$)	Main RFT%	Flexure RFT
	1	NACH			No		17 Ø 16
	2	NAE_1H			0.5	H	17 Ø 16
	3	NAE_2H			0.75		17 Ø 16
G1	4	NAE_3H	NWC	Non	1.0		17 Ø 16
	5	NACU			No		10 Ø 16
	6	NAE_1U			0.5	*U*	10 Ø 16
	7	NAE_2U			0.75		10 Ø 16
	8	NAE_3U			1.0		10 Ø 16
	9	NFCH			No		17 Ø 16
	10	NFE_1H			0.5	H	17 Ø 16
	11	NFE_2H			0.75		17 Ø 16
G2	12	NFE_3H	NWC	500°	1.0		17 Ø 16
	13	NFCU			No		10 Ø 16
	14	NFE_1U			0.5	*U*	10 Ø 16
	15	NFE_2U			0.75		10 Ø 16
	16	NFE_3U			1.0		10 Ø 16
	17	LACH			No		17 Ø 16
	18	LAE_1H			0.5	H	17 Ø 16
	19	LAE_2H			0.75		17 Ø 16
G3	20	LAE_3H	LWC	Non	1.0		17 Ø 16
	21	LACU			No		10 Ø 16
	22	LAE_1U			0.5	*U*	10 Ø 16
	23	LAE_2U			0.75		10 Ø 16
	24	LAE_3U			1.0		10 Ø 16
	25	LFCH			No		17 Ø 16
	26	LFE_1H			0.5	H	17 Ø 16
	27	LFE_2H			0.75		17 Ø 16
G4	28	LFE_3H	LWC	500°	1.0		17 Ø 16
	29	LFCU			No		10 Ø 16
	30	LFE_1U			0.5	*U*	10 Ø 16
	31	LFE_2U			0.75		10 Ø 16
	32	LFE_3U			1.0		10 Ø 16

N * normal-weight concrete, L * lightweight concrete, A * without fire, F * exposed to fire, C * under concentric load, E_1 *, E_2 * and E_3 * under eccentric load $(e/t) = 0.5$, 0.75 and 1.0 respectively, U * 0.4% rft from gross area of slab, H * 0.7% rft from gross area of slab.

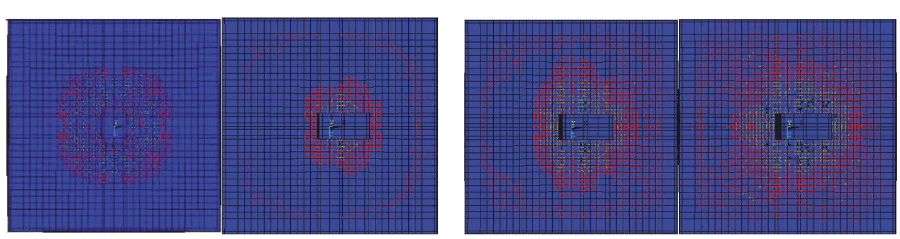

(a) (b) (c) (d)

Figure 4: Crack propagation before failure from the finite element model. (a) $e/t = 0$. (b) $e/t = 0.5$. (c) $e/t = 0.75$. (d) $e/t = 1.0$.

In case of high RFT percentage equal to 0.7%, the effect of applying the concentric and the changing eccentric vertical load LAE_1H, LAE_2H and LAE_3H with $e/t = 0.5$, 0.75, and 1.0, respectively, on the behavior of lightweight RC flat slabs was noted as the following.

It is clear from Figures 5 and 6, when applying the eccentric vertical load LAE_1H, LAE_2H, and LAE_3H with $e/t = 0.5$, 0.75, and 1.0, respectively, on the tested specimens with high RFT% that the ultimate load decreased compared to a concentric control specimen (LACH) by percentage 11.59%, 30.19%, and 44.15%, respectively, and the deflection corresponding to the ultimate load decreased with percentage 23.44%, 28.43% and 34.16%, respectively. It is also noted that the stiffness of these tested specimens increased by increasing the eccentric vertical load, although the stiffness of the eccentric specimen with $e/t = 1.0$ becomes similar to concentric control specimen, as shown in Figure 5.

In case of usual RFT percentage equals to 0.4%, the effect of applying the concentric and the changing eccentric vertical load LAE_1U, LAE_2U, and LAE_3U with $e/t = 0.5$, 0.75, and 1.0, respectively, on the behavior of a lightweight RC flat slab was noted as shown in figures 5 to 8.

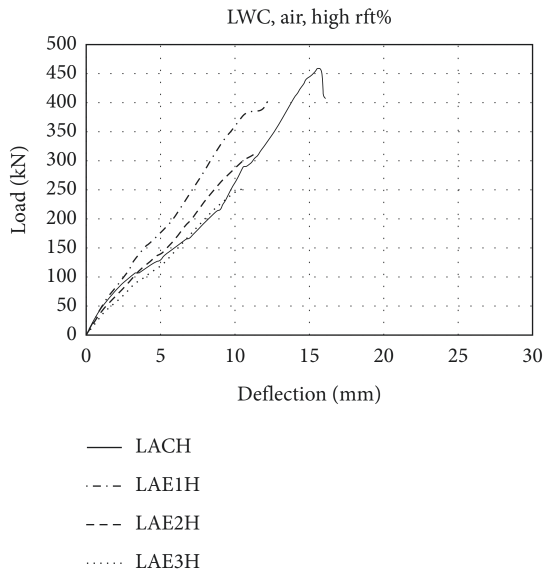

FIGURE 5: Effect of e/t ratio on the load-deflection curves for LWC with high RFT%.

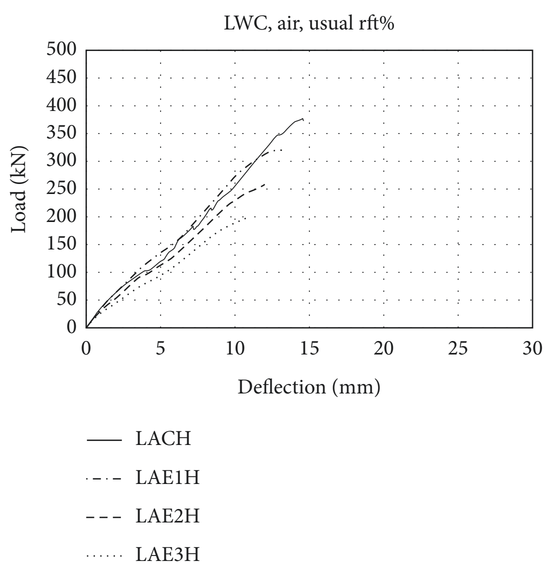

FIGURE 6: Effect of e/t ratio on the load-deflection curves for LWC with usual RFT%.

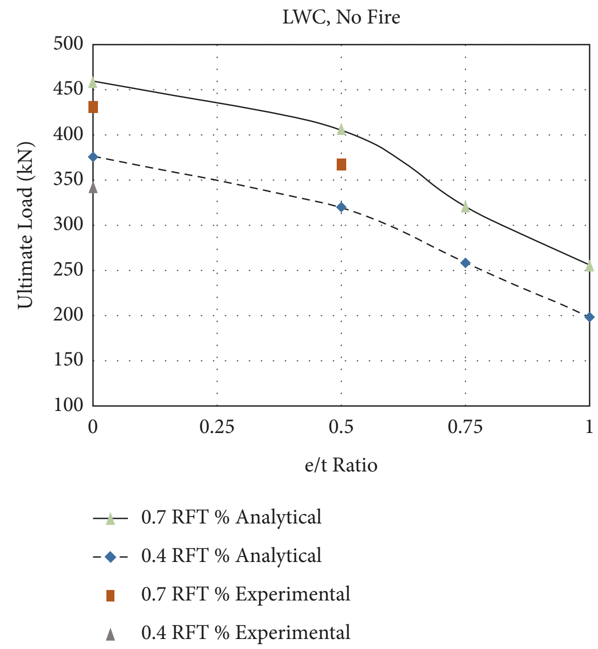

FIGURE 7: Effect of e/t ratio on load for LWC the ultimate.

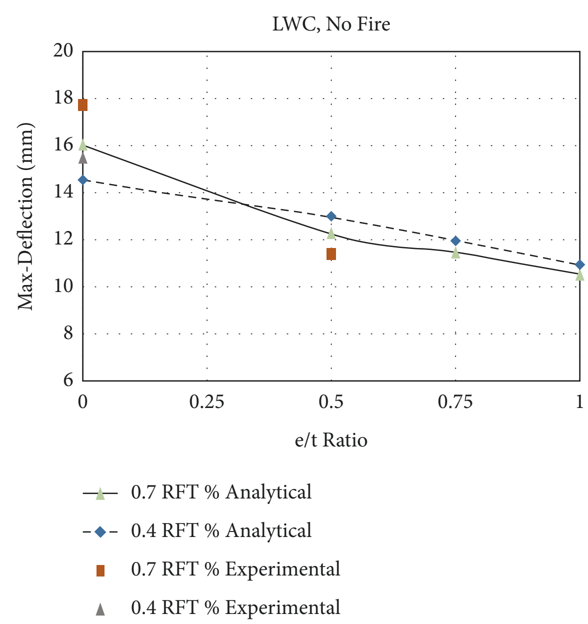

FIGURE 8: Effect of e/t ratio on the maximum deflection for LWC.

It is clear from Figures 7 and 8, when applying the eccentric vertical load LAE_1U, LAE_2U, and LAE_3U with $e/t = 0.5$, 0.75, and 1.0, respectively, on the tested specimens with usual RFT% that the ultimate load decreased compared to concentric control specimen (LACU) by percentage 15.10%, 31.40%, and 47.27%, respectively, and the deflection corresponding to the ultimate load decreased with percentage 10.65%, 17.73%, and 24.74%, respectively. It is also noted that the stiffness of these tested specimens increased by increasing the eccentric vertical load, although the eccentric specimen with $e/t = 0.5$ have the same stiffness of concentric control specimen as shown in Figure 7.

On studying the behavior of lightweight RC, flat slabs which had been exposed to fire with RFT percentages equal to 0.7% and 0.4% when applying the concentric and changing eccentric vertical load $e/t = 0.5$, 0.75 and 1.0.

4.3.1. Discussion for Specimens with High RFT Percentage Equal to 0.7%, e/t (0 to1) and Exposed to Fire. Figures 9 and 10 illustrate that when applying the eccentric vertical load LFE_1H, LFE_2H, and LFE_3H with $e/t = 0.5$, 0.75, and 1.0, respectively, on the tested specimens were exposed to fire with high RFT% that the ultimate load decreased comparing to concentric control specimen (LFCH) by percentage 20.24%, 44.10%, and 61.58%, respectively. The corresponding deflection to the ultimate load decreases with

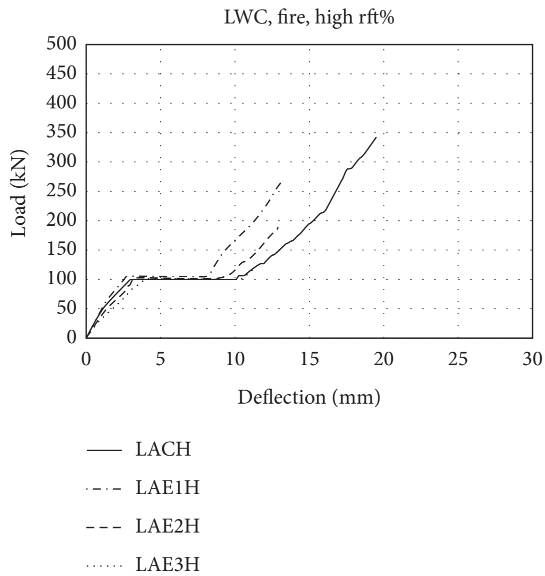

Figure 9: Effect of *e*/*t* ratio on the load-deflection curves for LWC with high RFT% when exposed to fire.

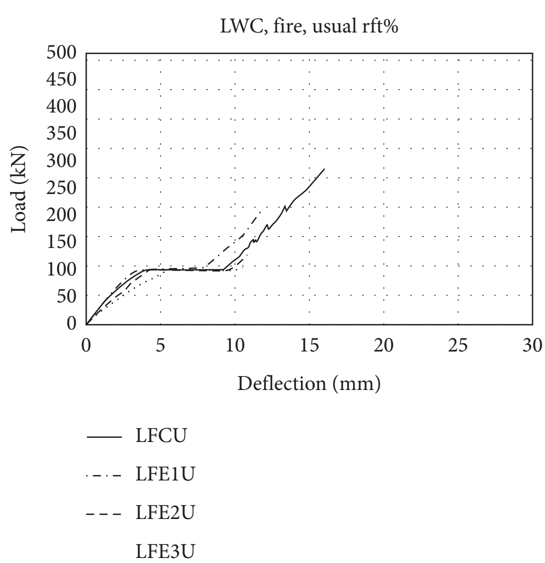

Figure 10: Effect of *e*/*t* ratio on the load-deflection curves for LWC with usual RFT% when exposed to fire.

percentage 31.94%, 33.28%, and 38.58%, respectively. The stiffness of those tested specimens increased by increasing the eccentricity, although the stiffness of the eccentric specimen with $e/t = 1.0$ becomes similar to concentric control specimen as shown in Figure 9.

4.3.2. Discussion for Specimens with Usual RFT Percentage Equal to 0.4%, e/t (0 to1) and Exposed to Fire. Figures 9 and 10 illustrate that the applying eccentric vertical load LFE_1U, LFE_2U, and LFE_3U with $e/t = 0.5$, 0.75, and 1.0, respectively, on the tested specimens which exposed to fire with usual

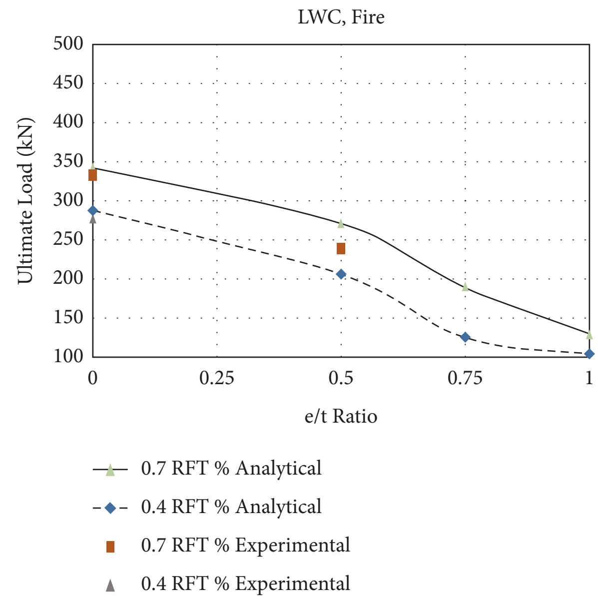

Figure 11: Effect of *e*/*t* ratio on the ultimate load for LWC when exposed to fire.

RFT% that will cause a decreasing in the ultimate load when comparing it to the concentric control specimen (LFCU) by percentage 27.76%, 55.94%, and 63.20%, respectively. Also, the corresponding deflection to the ultimate load decreases with percentage 26.96%, 32.79%, and 34.29%, respectively.

The stiffness of these tested specimens will be increased by increasing the eccentric vertical load, although the eccentric specimen with $e/t = 0.5$ have the same stiffness of concentric control specimen as shown in Figures 11 and 12.

For more clarification, Figure 13 presents the relation between variation of eccentricity(e/t) and deflection during the fire process with a constant load for LWC specimens at high and usual RFT% (0.7% and 0.4%, respectively). Related to the control specimen (LFCH), the deflection of high RFT % decreased by approximately 16.5%. Similarly for control specimen (LFCU), the deflection of usual RFT% decreased by approximately 13.3%.

5. Comparison of Parametric Study Database-Ultimate Loads and Loads from Different Codes Using the Proposal Factors for ACI 318 and BS 8110

Related to the experimental tests, reduction factors of concrete compressive strength in foam concrete depending on the reduction factors in lightweight concrete strength have been proposed by Riad and Shoeib [18]. In addition to, reduction factors in compressive strength of lightweight concrete exposed to 500°C fire for ACI-318 and BS-8110 codes were also proposed. This part discusses the comparison between the results of the finite element analysis, experimental tests, and different codes (ACI 318 and BS 8110) related to the mentioned reduction factors.

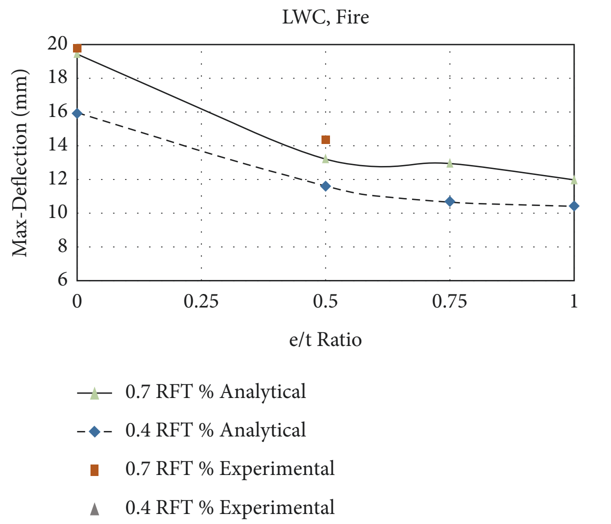

Figure 12: Effect of *e*/*t* ratio on the maximum deflection for LWC when exposed to fire.

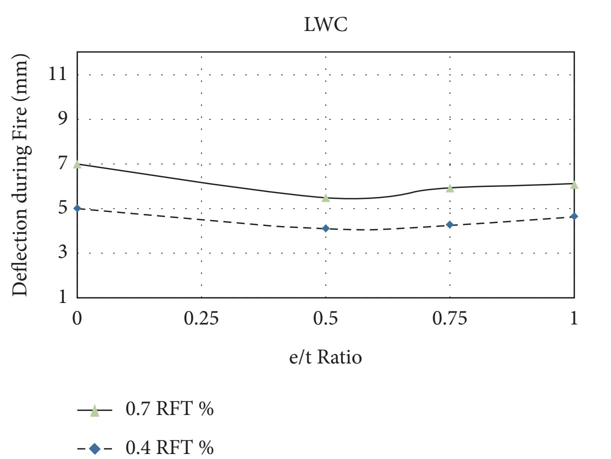

Figure 13: Effect of e/*t* ratio on the deflection during fire process at constant load for LWC.

Figure 14 appears in case LWC specimens were not exposed to fire by using the proposal reduction factors for ACI-318 and BS-8110 codes, the prediction load closes to database-ultimate loads by average percentage 24.0% and 16.25%, respectively, compared to the load using the reduction factors of these codes when increased *e*/*t* ratio to 0.5, 0.75, and 1.0. Figure 15 shows the comparison between the fired LWC database-ultimate loads and different codes which using the proposal factors.

Moreover, in case of LWC specimens that were exposed to fire, by using the proposal reduction factors for ACI-318 and BS-8110 codes, the prediction load closed to database-ultimate loads by an average percentage of 18.6% and 12.4%, respectively, compared to the load using the reduction factors of these codes when increased *e*/*t* ratio to 0.5, 0.75, and 1.0 as shown before in Figures 5–8.

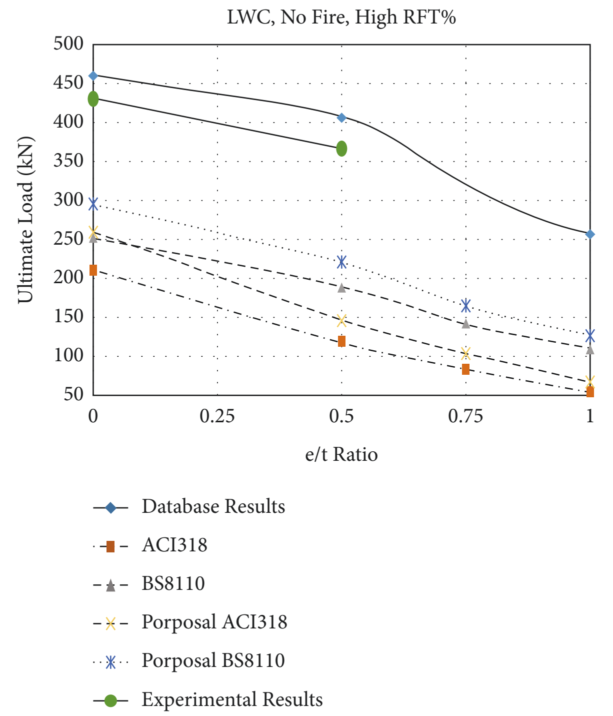

Figure 14: Comparison of LWC database-ultimate loads and different codes using the proposal factors.

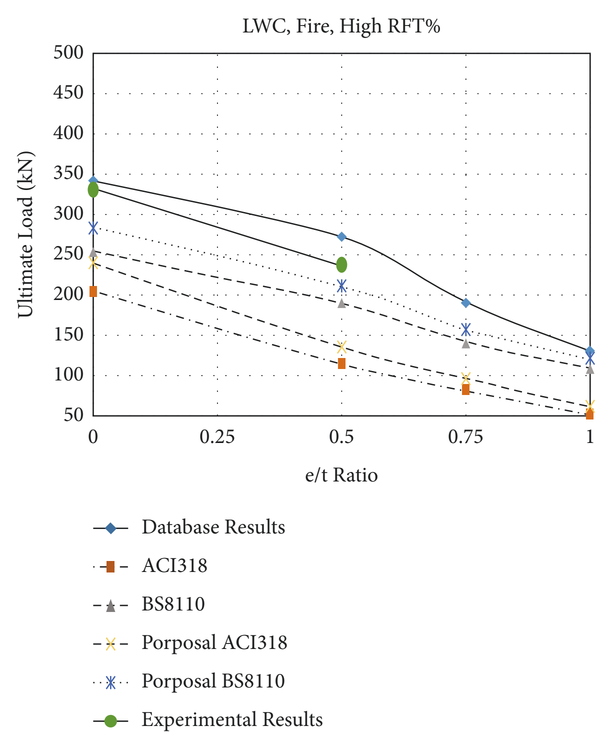

Figure 15: Comparison of fired LWC database-ultimate loads and different codes using the proposal factors.

6. Conclusion

The main purpose of this study is to identify the efficiency of structural lightweight polystyrene foam concrete flat slabs when these slabs are exposed to fire by the finite element method. In this study, reinforced foam concrete flat slabs were exposed to fire under eccentric and concentric loads. The validity of the adopted models was verified through comparison with a previous experimental study which has been conducted by Riad and Shoeib [18]. By using the software analysis (ANSYS), crack patterns, load-deflection curves, steel strains, and deflection during the fire were analyzed in this study. The following are concluded in this work:

(1) The density of lightweight structural concrete that was produced using fibers and additives was 1820 kg/m^3, and the compressive strength of concrete reached 30.0 MPa.

(2) When comparing the behavior of lightweight structural flat slabs which manufactured using polystyrene foam with that of normal-weight concrete flat slabs, we found the following:

  (i) The maximum load was low in the lightweight foam concrete slab with rates ranging from 7.0% to 4% for concentric load and eccentric load, respectively; this is compared to the maximum load of normal-weight concrete.

  (ii) A decrease in the number of cracks in lightweight foam concrete as well as an increase in the width of cracks was observed.

  (iii) When calculating the theoretical punching shear force in ACI-318 and BS-8110 codes, the proposed modification factors of foam concrete can be equal to 1.24 and 1.163, respectively.

(3) By comparing the behavior of the structural lightweight polystyrene foam concrete flat slab and normal-weight concrete flat slab exposed to fire, we find that:

  (i) A decrease in the maximum load of foam concrete and normal-weight concrete was observed by 25% and 13%, respectively.

  (ii) The recommended reduction factors in compressive strength according to ACI-318 and BS-8110 codes are 0.68 and 0.56 instead to 0.82 and 0.70, respectively.

(4) It is highly recommended to study more specimens with different types of foams and fibers.

Data Availability

The data used to support the findings of this study are included within the article and are available from the corresponding authors on reasonable request.

Conflicts of Interest

The authors declare that they have no conflicts of interest.

Authors' Contributions

Dr Ahmed Ehab and Dr Magdy Riad collected the data, conceived, and designed the analysis. Dr Ahmed. M. Yosri, Dr Mohamed Farouk, Dr. Mohamed Abdelmongy, and Dr Majed Alzara have performed the analyses, validated, discussed the results, and wrote the paper. All authors discussed the results and contributed to the final manuscript.

References

[1] M. Tech Scholar, "Experimental study on foam concrete," *International Journal of Civil, Structural, Environmental and Infrastructure Engineering Research and Development*, vol. 4, no. 1, pp. 145–158, 2014.

[2] A. A. Hilal, N. H. Thom, and A. R. Dawson, *Foamed Concrete: From Weakness to Strength, 34th Cement and Concrete Science Conference*, University of Sheffield, Sheffield, UK, 2014.

[3] M. H. Wan lbrahim, N. Jamaluddin, J. M. Irwan, P. J. Ramadhansyah, and A. Suraya Hani, "Compressive and flexural strength of foamed concrete containing polyolefin fibers," *Advanced Materials Research*, vol. 91 I, pp. 489–493, 2014.

[4] Y. Lee, H. Limjee, S. K. Lim, and C. S. Tan, "Flexural Behavior of Reinforced Lightweight Foamed Mortar Beams and Slab," *KSCE Journal of Civil Engineering*, pp. 1817–1822, 2017.

[5] EN 1992-1-1, "Eurocode 2: design of concrete structures—Part 1–1: general rules and rules for buildings," British Standard Institution, London, UK, Incl. Corrigendum 1: EN 1992-1-1:2004/AC:2008, 2014.

[6] B. Fédération Internationale Du, *Fib Model Code for Concrete Structures 2010*, Fédération Internationale Du Béton, Lausanne, Switzerland, 2013.

[7] ACI-318-19, "ACI Committee 318; Building Code Requirements for Structural Concrete (ACI 318–19) and Commentary on Building Code Requirements (ACI 318-19)," American Concrete Institute: Farmington Hills, MI, USA, ACI-318-19, 2019.

[8] Aci-318, "Building Code Requirements for Structural concrete (ACI 318) and Commentary ACI -318R," Aci-318, p. 369, American Concrete Institute, MI, USA, 2008.

[9] BS-8110, "British Standard of Structural Use of concrete - Part 2: Code of Practice for Special Circumstances," Board of BSI, London, UK, BS-8110-2, 2005.

[10] J. Hulimka, K. Rafał, and J. Agnieszka, "Laboratory Tests of Foam concrete Slabs Reinforced with Composite Grid," *Elsevier, Procedia Engineering*, pp. 337–344, 2017.

[11] S. J. George, "Structural Performance of Reinforced Concrete Flat Plat Buildings Subjected to Fire," UNLV Theses, Dissertations, Professional Papers, and Capstones, Nevada, Las Vegas, 2012.

[12] O. Kalmykov, "Study of fire-resistance of reinforced concrete slab of a new type," *MATEC Web of Conferences*, vol. 116, 2017.

[13] S. F. El-Fitiany and M. A. Youssef, "Assessing the flexural and axial behavior of reinforced concrete members at elevated temperatures using sectional analysis," *Fire Safety Journal*, vol. 44, pp. 691–703, 2009.

[14] G. Wang, *Performance of Reinforced concrete Flat Slabs Exposed to Fire*, Master of Engineering, University of Canterbury, Christchurch, New Zealand, University of Canterbury, 2004 .

[15] B. Wang, Y. Dong, and L. Gao, "Fire Experimental Study of Four-Edge Fixed Reinforced concrete Slab in Fire," *Advanced Materials Research*, vol. 163–167, 2011.

[16] P. J. Moss, R. P. Dhakal, G. Wang, and A. H. Buchanan, "The fire behaviour of 17. multi-bay, two-way reinforced concrete slabs. Engineering Structures," vol. 30, no. 12, 2008.

[17] I. A. Fletcher, S. Welch, J. L. Torero, and A. Usmani, "Behavior of concrete structures in fire," *Thermal Science*, vol. 11, no. 2, pp. 37–52, 2007.

[18] M. Riad and S. Ata El-kareim Shoeib, "Behavior of structural lightweight polystyrene foam concrete flat slabs when exposed to fire," *The Open Construction & Building Technology Journal*, 2018.